whereas in the case of **10** as well as for the resonances of the methylene carbon atoms of the atrane cage of both molecules, this effect is too small to be detected.

Conclusions. The new ligand **3b** is easily accessible via diphosphination of the azasilatrane precursor **1c**. The chemical reactivity of **3b** was found to be typical of tertiary phosphines, thus allowing facile alkylation, oxidation with sulfur, and complexation. The coordination compounds synthesized displayed two modes of attachment of the ligand to the metal center, with **3b** behaving as either a bidentate (P,P′ coordination) or tridentate (P,P′,O coordination) ligand. The latter mode represents the first example of metal coordination by a silatranyl ether group, and it is favored by both the chelate effect and the enhanced basicity at oxygen due to the transannular $N_{ax}\rightarrow Si$ bond. The results of NMR spectroscopic studies in both solution and the solid state are consistent with the preservation of a transannular $N_{ax}\rightarrow Si$ bond in all cases, with an increase in bond strength being observed as a consequence of either coordination of the axial oxygen atom to a metal center or accumulation of positive charge in the atrane cage.

Acknowledgment. J.G.V. thanks the AFOSR for a grant supporting this work. The crystal structure determinations were carried out at the Iowa State Molecular Structure Laboratory. We are grateful to the W. R. Grace Co. for a generous research sample of tren.

Supplementary Material Available: Description of the structure solution of **7** and tables of positional and anisotropic thermal parameters, bond lengths, least-squares planes, and bond angles for **5b** and **7** (20 pages); tables of calculated and observed structure factors (26 pages). Ordering information is given on any current masthead page.

Synthesis, Structure, and Properties of Dicarbonyl Bis(phosphine) 1,4-Diphenyltetraazabutadiene Complexes of Molybdenum and Tungsten

Soon W. Lee and William C. Trogler*

Department of Chemistry, D-006, University of California at San Diego, La Jolla, California 92093-0506

Received September 14, 1989

The complexes $MoBr_2(CO)_2(PPh_3)_2$ and $MoBr_2(CO)_2(PEt_3)_2$ react with $[Li(THF)_x]_2[PhNN{=}NNPh]$ ($[Li(THF)_x]_2$(I)) to yield crystalline materials of formula $Mo(N(Ph)N{=}NNPh)(CO)_2(PPh_3)_2{\cdot}C_6H_6$ (III) and $Mo(N(Ph)N{=}NNPh)(CO)_2(PEt_3)_2$ (IV), respectively. The complex *trans*-$WBr_2(CO)_2(PPh_3)_2$ reacts with $[Li(THF)_x]_2[PhNN{=}NNPh]$ ($[Li(THF)_x]_2$(I)) to yield *trans*-$W(PPh_3)_2(CO)_4$ and the cyclic tetrazene complex $W(N(Ph)N{=}NNPh)(CO)_2(PPh_3)_2{\cdot}C_6H_6$ (IIIa). Dibromotetracarbonyltungsten reacts with 3 mol of PMe_3 to give $WBr_2(CO)_2(PMe_3)_3$ (IIa). Complex IIa reacts with I to exclusively yield $W(N(Ph)N{=}NNPh)(CO)_2(PMe_3)_2$ (IVa). The crystal structures of IIa, III, IIIa, IV, and IVa were determined through X-ray diffraction at room temperature: complex III crystallizes in the monoclinic crystal system, space group $C2$, with lattice constants a = 20.675 (8) Å, b = 9.946 (4) Å, c = 15.285 (9) Å, β = 130.54 (3)°, and Z = 2; IV crystallizes in the tetragonal system, space group $P4_32_12$, with lattice constants a = 13.000 (3) Å, c = 17.941 (6) Å, and Z = 4; IIa crystallizes in the orthorhombic system, space group $Pbca$, with lattice constants a = 8.938 (4) Å, b = 15.416 (5) Å, c = 29.974 (9) Å, and Z = 8; IIIa crystallizes in the monoclinic system, space group $C2$, with lattice constants a = 20.598 (10) Å, b = 9.976 (5) Å, c = 15.257 (7) Å, β = 130.49 (3)°, and Z = 2; IVa crystallizes in the monoclinic system, space group $P2_1$, with lattice constants a = 9.476 (3) Å, b = 11.902 (3) Å, c = 10.473 (3) Å, β = 90.93 (2)°, and Z = 2. Least-squares refinement of the structures led to R factors of 0.047 (III), 0.034 (IV), 0.048 (IIa), 0.059 (IIIa), and 0.072 (IVa). The coordination spheres of molybdenum and tungsten in III, IIIa, IV, and IVa can be described as distorted octahedrons with trans PR_3 groups. Complex IIa exhibits a monocapped-octahedral structure based on a *fac*-$WBr_2(CO)(PMe_3)_3$ group (bromines trans to two P) with CO capping the face defined by the three P atoms. This structure is maintained in solution as evidenced by a doublet and triplet in the ^{31}P NMR spectrum at δ −15.2 and −38.7, respectively, with J_{P-P} = 14.6 Hz. Complexes III, IIIa, IV, and IVa have formal 18-electron configurations if the tetraazabutadiene ligand is viewed as a neutral four-electron donor analogous to the diazabutadiene ligand. The structures of III, IIIa, IV, and IVa show a progressive increase in distortion from octahedral symmetry as the PR_3 groups become smaller. The distortion rotates the MN_4 metallacycle plane out of coplanarity with the two CO groups by as much as 30°. Electrochemical studies show that IV displays two reversible one-electron reductions. Electrochemical studies of IVa reveal only irreversible reduction processes. Complexes IV and IVa do not react with small two-electron-donating molecules (CO, PMe_3, and CH_3CN).

Introduction

Transition-metal complexes that have unsaturated metallacycles containing the 1,4-disubstituted tetraazabutadiene ligand (also called tetraazadiene, tetrazene, or tetrazenido) have attracted interest because of their novel bonding features.[1] Attention has focused on the delo-

0276-7333/90/2309-1470$02.50/0

calization of π-electron density in the metallacycles and the role of the metal d orbitals in bonding. For example, studies on the redox chemistry of $CpCo(1,4\text{-}R_2N_4)$ (R = CH_3, C_6H_5, C_6F_5, 2,4-$F_2C_6H_3$, 2,6-$Me_2C_6H_3$; Cp = η^5-C_5H_5) showed that tetraazabutadiene ligands are strong π-acceptor groups that can be used to stabilize electron-rich 19-electron organometallic complexes.[1e] Since 1967 several transition-metal tetrazene complexes have been reported, including derivatives of Co, Rh, Ir, Fe, Ni, and Pt.[1] They have been prepared by coupling reactions between either an organic azide (RN_3) or a diazonium salt (RN_2^+) and a late-transition-metal complex in a low oxidation state. Because only late-transition-metal complexes have been prepared (to the right of the manganese triad) and because tetrazene ligands are known as good π-acceptor groups, it has been believed that metal to ligand π-back-bonding plays an important role in stabilizing the complexes.

Recently we reported the preparation of tetrazene complexes of group VIII metals (Ni, Pd, and Pt) from the readily available tetrazenido dianion (I), which is prepared by nonoxidative N–N bond formation (eq 1).[2] This ligand

$$\mathrm{PhNHLi} + \mathrm{PhN_3} \rightleftharpoons \mathrm{Ph(H)NN{=}NN(Ph)Li} \xrightarrow{{}^{n}\mathrm{BuLi}} \underset{\mathrm{Li_2(I)}}{\mathrm{Ph(Li)NN{=}NN(Ph)Li}} \quad (1)$$

has also permitted the synthesis of main-group tetrazene complexes of Si and Ge.[3] In this paper we report the synthesis, structure, and properties of the first early-transition-metal tetraazabutadiene complexes $M(1,4\text{-}Ph_2N_4)(CO)_2(PR_3)_2$ (M = Mo, W; PR_3 = PPh_3, PEt_3, PMe_3). We also report the synthesis and structure of the seven-coordinate tungsten complex $WBr_2(CO)_2(PMe_3)_3$.

Experimental Section

Reactions were performed with standard Schlenk and cannula filtration techniques under a nitrogen atmosphere. Solids were manipulated under nitrogen in a Vacuum Atmospheres glovebox equipped with an HE-493 Dri-Train. Glassware was flame-dried or oven-dried before use. Benzene, ethers, and hydrocarbon solvents were refluxed over sodium or potassium benzophenone ketyl and distilled under nitrogen or by vacuum transfer. Dichloromethane was distilled from CaH_2. Benzene-d_6 was freeze–pump–thaw-degassed before use and stored under nitrogen. The dianionic reagent $[Li(THF)_x]_2[PhNN{=}NNPh]$ ($[Li(THF)_x]_2(I)$)[2] $WBr_2(CO)_2(PPh_3)_2$, and $MoBr_2(CO)_2(PPh_3)_2$[4] were prepared by literature methods. $MoBr_2(CO)_2(PEt_3)_2$ was prepared by modification of literature methods.[5,6] Tungsten and molybdenum hexacarbonyls, triphenylphosphine, triethylphosphine, and bromine were purchased from commercial sources and used without purification.

Cyclic voltammetric studies were carried out with the use of a BAS 100 electrochemical analyzer equipped with a Houston Instruments DMP-40 plotter. Solutions (THF) were ca. 1 mM in the metal complex and contained 0.1 M $[Bu_4N][PF_6]$ supporting electrolyte. For these measurements, a conventional three-electrode cell (Pt-disk working electrode, Pt-wire auxiliary electrode, Ag-wire pseudo reference electrode) was employed. Instrumental *iR* compensation was applied for all measurements. The $E^{\circ\prime}$ value for the Cp_2Fe/Cp_2Fe^+ couple was 0.62 V at a 300 mV/s scan rate in this cell. IR spectra were recorded with an IBM IR/32 FTIR spectrometer. EPR measurements were performed on a Varian E-3 X-band 9.546-GHz spectrometer at room temperature. Magnetic field strength was calibrated by use of diphenylpicrylhydrazyl (DPPH) as standard (g = 2.0037). UV spectra were obtained with use of an IBM UV 9420 spectrometer. ^1H and ^{31}P NMR spectra were obtained with either a Varian EM-390 or a General Electric QE 300-MHz spectrometer. Elemental analyses were performed by Schwarzkopf Microanalytical Laboratory.

Synthesis of Dibromodicarbonylbis(triethylphosphine)molybdenum(II), $MoBr_2(CO)_2(PEt_3)_2$ (II). To 7.0 g (18.6 mmol) of *cis*-$Mo(CO)_4(NHC_5H_{10})_2$[5] in 60 mL of CH_2Cl_2 was added 6 mL (40.8 mmol) of triethylphosphine (PEt_3). After it was refluxed for 1 h, the slurry was filtered through Celite to yield an orange solution. The solvent was removed under vacuum, and 10 mL of CH_3OH was added to the oily residue to form white crystals. The solution was allowed to stand at −40 °C overnight to yield (6.3 g, 76%) white crystals of *cis*-$Mo(CO)_4(PEt_3)_2$. The 6.3 g (14.2 mmol) of *cis*-$Mo(CO)_4(PEt_3)_2$ was dispersed in 50 mL of CCl_4, and 2.6 g (16.2 mmol) of Br_2 in 20 mL of CCl_4 was added dropwise. After 15 min the solvent was removed and 15 mL of CH_3OH was added to the oily residue to form a yellow solid of $MoBr_2(CO)_3(PEt_3)_2$. The solution was allowed to stand at −40 °C overnight. The yellow solid was filtered and dissolved in 40 mL of CH_2Cl_2, and the solution was refluxed for 1 h. The resulting blue solution was concentrated, and 60 mL of diethyl ether was added to yield 3.40 g of blue $MoBr_2(CO)_2(PEt_3)_2$. An additional yield (1.86 g) was obtained by slow cooling of the ether filtrate to −40 °C. The overall yield is 68%. Mp: 113–115 °C (lit.[6] mp 117–121 °C). IR (ν_{CO}, KBr): 1854, 1939 cm^{-1}.

Synthesis of Dicarbonyl(1,4-diphenyltetraazabutadiene)bis(triphenylphosphine)molybdenum, $Mo(N(Ph)N{=}NNPh)(CO)_2(PPh_3)_2{\cdot}C_6H_6$ (III). Addition of 0.3 g of $[Li(THF)_x]_2(I)$ in 30 mL of benzene to a stirred blue slurry of 0.5 g (0.60 mmol) of *trans*-$MoBr_2(CO)_2(PPh_3)_2$ in 30 mL of benzene gave a red solution after 4 h. The solution was filtered, concentrated under vacuum, and layered with pentane to yield a ~1:1 mixture of green crystalline III and yellow crystals of *cis*-$Mo(CO)_4(PPh_3)_2$, whose IR spectrum agreed with that in the literature.[7] IR (ν_{CO}, KBr) for III: 1826, 1925 cm^{-1}. Green crystalline III was hand-separated for X-ray and IR analysis.

Synthesis of Dicarbonyl(1,4-diphenyltetraazabutadiene)bis(triethylphosphine)molybdenum, $Mo(N(Ph)N{=}NNPh)(CO)_2(PEt_3)_2$ (IV). Addition of 0.4 g of $[Li(THF)_x]_2(I)$ in 30 mL of benzene to a stirred solution of 0.4 g (0.73 mmol) of $MoBr_2(CO)_2(PEt_3)_2$ in 30 mL of benzene gave a red solution after 6 h. The solvent was removed under vacuum. The residue was extracted with 60 mL of warm heptane, and the filtrate was concentrated to saturation and cooled slowly to −40 °C to yield a red solid (0.09 g, 20.6%) of IV. ^1H NMR (C_6D_6): δ 7.74–7.09 (m, C_6H_5), 3.26 (q, CH_2, $J_{H\text{-}H}$ = 7.0 Hz, $^2J_{P\text{-}H}$ = 14.0 Hz), 1.11 (t, CH_3, $J_{H\text{-}H}$ = 7.0 Hz). $^{31}P\{^1H\}$ NMR (C_6D_6): δ 39.6 (s) UV (C_6H_6): 561 nm (490 M^{-1} cm^{-1}), 416 nm (5800 M^{-1} cm^{-1}), 322 nm (5600 M^{-1} cm^{-1}, sh). IR: (ν_{CO}, KBr): 1815, 1910 cm^{-1}. Anal. Calcd for $C_{26}H_{40}N_4O_2P_2Mo$: C, 52.18; H, 6.74; N, 9.36. Found: C, 51.73; H, 6.27; N, 9.46. Mp: 152–164 °C with liberation of gas.

Synthesis of Dibromodicarbonyltris(trimethylphosphine)tungsten(II), $WBr_2(CO)_2(PMe_3)_3$ (IIa). Finely ground $W(CO)_6$ (5 g, 14.25 mmol) was suspended in 60 mL of

(1) (a) Gross, M. E.; Trogler, W. C.; Ibers, J. A. *J. Am. Chem. Soc.* **1981**, *103*, 192. (b) Trogler, W. C.; Johnson, C. E.; Ellis, D. E. *Inorg. Chem.* **1981**, *20*, 980. (c) Gross, M. E.; Trogler, W. C. *J. Organomet. Chem.* **1981**, *209*, 407. (d) Johnson, C. E.; Trogler, W. C. *J. Am. Chem. Soc.* **1981**, *103*, 6352. (e) Maroney, M. J.; Trogler, W. C. *Ibid.* **1984**, *106*, 4144–4151. (f) Overbosch, P.; van Koten, G.; Overbeek, O. *Ibid.* **1980**, *102*, 2091. (g) Doedens, R. J. *Chem. Commun.* **1968**, 1271. (h) Einstein, F. W. B.; Sutton, D. *Inorg. Chem.* **1972**, *11*, 2827. (i) Overbosch, P.; van Koten, G.; Grove, D. M.; Speck, A. L.; Duisenberg, A. J. M. *Ibid.* **1982**, *21*, 3253. (j) Cenini, S.; Fantucci, P.; La Monica, G. *Inorg. Chim. Acta* **1975**, *13*, 243. (k) La Monica, G.; Sondrinic, P.; Zingales, F.; Cenini, S. *J. Organomet. Chem.* **1973**, *50*, 287. (l) Overbosch, P.; van Koten, G.; Speck, A. L.; Roelofsen, G.; Duisenberg, A. J. M. *Inorg. Chem.* **1982**, *21*, 3908. (m) Geisenberger, J.; Nagel, V.; Sebald, A.; Beck, W. *Chem. Ber.* **1983**, *16*, 911. (n) Moore, D. S.; Robinson, S. D. *Adv. Inorg. Chem. Radiochem.* **1986**, *30*, 1.

(2) (a) Lee, S. W.; Miller, G. A.; Campana, C. F.; Trogler, W. C. *J. Am. Chem. Soc.* **1987**, *109*, 5050. (b) Lee, S. W.; Miller, G. A.; Campana, C. F.; Maciejewski, M. L.; Trogler, W. C. *Inorg. Chem.* **1988**, *27*, 1215.

(3) Miller, G. A.; Lee, S. W.; Trogler, W. C. *Organometallics* **1989**, *8*, 738.

(4) Colton, R.; Tomkins, I. B. *Aust. J. Chem.* **1966**, *19*, 1519.

(5) Darensbourg, D. J. *Inorg. Chem.* **1979**, *18*, 14.

(6) (a) Moss, J. R.; Shaw, B. L. *J. Chem. Soc. A* **1970**, 595. (b) Anker, M. W.; Colton, R.; Tomkins, I. B. *Aust. J. Chem.* **1967**, *20*, 9.

(7) Darensbourg, D. J.; Kump, R. L. *Inorg. Chem.* **1978**, *17*, 2680.

Table I. Crystallographic Data and Summary of Data Collection and Structure Refinement

	IIa	III	IIIa	IV	IVa
formula	$C_{11}H_{27}O_2P_3Br_2W$	$C_{56}H_{46}N_4O_2P_2Mo$	$C_{56}H_{46}N_4O_2P_2W$	$C_{26}H_{40}N_4O_2P_2Mo$	$C_{20}H_{28}N_4O_2P_2W$
fw	627.96	964.94	1052.85	598.58	602.31
cryst syst	orthorhombic	monoclinic	monoclinic	tetragonal	monoclinic
space group	*Pbca*	*C*2	*C*2	$P4_32_12$	$P2_1$
a, Å	8.938 (4)	20.675 (8)	20.598 (10)	13.000 (3)	9.476 (3)
b, Å	15.416 (5)	9.946 (4)	9.976 (5)		11.902 (3)
c, Å	29.974 (9)	15.285 (9)	15.257 (7)	17.941 (6)	10.473 (3)
β, deg		130.54 (3)	130.48 (3)		90.93 (2)
V, Å^3	4130 (3)	2388 (2)	2384 (2)	3033 (2)	1181 (1)
d_{calc}, g cm^{-3}	2.02	1.34	1.47	1.31	1.69
μ, cm^{-1}	97.8	3.73	25.9	5.52	51.5
scan type	*ω*	*ω*–2*θ*	*ω*–2*θ*	*ω*–2*θ*	*ω*–2*θ*
no. of unique data	3101	1741	2309	3056	2172
no. of reflns used, $I > 3\sigma(I)$	1440	1487	2112	2207	1392
no. of params	107	110	110	147	110
transmission	0.58–0.97		0.40–0.48		0.49–0.75
Z	8	2	2	4	2
scan range, deg	$3 < 2\theta < 45$	$3 < 2\theta < 40$	$3 < 2\theta < 50$	$3 < 2\theta < 45$	$3 < 2\theta < 50$
largest resid peak, e Å^{-3}	1.2	0.39	1.9	0.38	5.3
R	0.048	0.047	0.055	0.034	0.072
R_w	0.070	0.056	0.071	0.047	0.088
GOF	0.704	1.51	0.96	1.08	1.04

CH_2Cl_2 cooled to −78 °C in an 2-propanol/dry ice bath. Bromine (2.5 g, 31.28 mmol) was added, and vigorous evolution of CO occurred. After 10 min the cold bath was removed and the solution was stirred for 30 min. The solvent was removed under vacuum, and the remaining red solid was redissolved in 100 mL of CH_2Cl_2. The dark red solution was filtered into a solution of 3 mL (29.5 mmol) of trimethylphosphine in 15 mL of CH_2Cl_2 at −78 °C. After 15 min the cold bath was removed and the solution was stirred for 5 h. Solvent was removed to yield a yellow solid. The product was recrystallized by cooling a concentrated diethyl ether solution to −40 °C to yield yellow crystalline IIa (3.82 g, 6.09 mmol, 42.7%). ^{1}H NMR (C_6D_6): δ 1.29–1.55 (m, CH_3). ^{31}P{^{1}H} NMR (C_6D_6): δ −15.2 (d, 2 P, $^2J_{P-P}$ = 14.6 Hz, J_{W-P} = 155 Hz), −38.7 (t, 1, P, $^2J_{P-P}$ = 14.6 Hz, J_{W-P} = 152 Hz). IR (ν_{CO}, mineral oil): 1819, 1919 cm^{-1}. UV (C_6H_6): 378 nm (1500 M^{-1} cm^{-1}), 336 nm (2000 M^{-1} cm^{-1}). Anal. Calcd for $C_{11}H_{27}O_2P_3Br_2W$: C, 21.04; H, 4.33. Found: C, 21.20; H, 4.38. Mp: 202–204 °C.

Synthesis of Dicarbonyl(1,4-diphenyltetraazabutadiene)bis(triphenylphosphine)tungsten, W(N(Ph)N=NNPh)(CO)$_2$(PPh$_3$)$_2$·C$_6$H$_6$ (IIIa). Addition of 0.3 g of $[Li(THF)_x]_2(I)$ in 30 mL of benzene to a stirred blue slurry of 0.4 g (0.34 mmol) of trans-$WBr_2(CO)_2(PPh_3)_2$ in 30 mL of benzene gave a red solution after 4 h. The solution was filtered, concentrated under vacuum, and layered with pentane to yield apparently a 1:1 mixture of green crystals of IIIa and yellow crystals of *trans*-$W(CO)_4(PPh_3)_2$ (ν_{CO} ($CHCl_3$) 1889 cm^{-1}).[8] IR (ν_{CO}, mineral oil) for IIIa: 1817, 1918 cm^{-1}. Crystals of IIIa were hand-separated for X-ray analysis.

Synthesis of Dicarbonyl(1,4-diphenyltetraazabutadiene)bis(trimethylphosphine)tungsten, W(N(Ph)N=NNPh)(CO)$_2$(PMe$_3$)$_2$ (IVa). Addition of 0.8 g of $[Li(THF)_x]_2(I)$ in 30 mL of toluene to a stirred yellow solution of 1.0 g (1.59 mmol) of IIa in 30 mL of toluene gave a red solution after 7 h. The solution was filtered, concentrated under vacuum, and cooled slowly to −40 °C to yield (0.18 g, 18.8%) red crystals of IVa. ^{1}H NMR (C_6D_6): δ 7–8 (m, C_6H_5), 0.85 (d, $^2J_{P-H}$ = 9.5 Hz), ^{31}P{^{1}H} NMR (C_6D_6): δ −16.9 (s, J_{W-P} = 249 Hz). IR (ν_{CO}, mineral oil): 1815, 1906 cm^{-1}. UV (C_6H_6): 366 nm (4200 M^{-1} cm^{-1}). Anal. Calcd for $C_{20}H_{28}N_4O_2P_2W$: C, 39.89; H, 4.69; N, 9.30. Found: C, 39.80; H, 4.81; N, 9.24. Mp: 106–108 °C with liberation of gas.

X-ray Structure Determinations. All X-ray data were collected with use of a Nicolet R3m/V automated diffractometer equipped with a Mo X-ray tube and a graphite crystal monochromator. Details on crystal and intensity data are given in Table I. The orientation matrix and unit cell parameters were determined from 20 machine-centered reflections with $15 < 2\theta < 30°$. Axial photographs were used to verify the unit cell choice. Intensities of three check reflections were monitored after every 100 reflections during data collection. Data were corrected for Lorentz and polarization effects. No absorption correction was applied to the Mo data; however, the intensities for the W data were empirically corrected with ψ-scan data. All calculations were carried out on a Microvax II computer with use of the SHELXTL PLUS program package.

A yellow crystal of IIa, shaped as a block, of approximate dimensions 0.3 × 0.3 × 0.4 mm, was used for crystal and intensity data. The unit cell parameters and systematic absences 0*kl* ($k = 2n + 1$), *h*0*l* ($l = 2n + 1$), and *hk*0 ($h = 2n + 1$) unambiguously indicated *Pbca* as the space group. The structure was solved by conventional heavy-atom methods. The W, Br, and P atom thermal parameters were anisotropic.

A green crystal of III, shaped as a block, of approximate dimensions 0.2 × 0.3 × 0.4 mm, was used for crystal and intensity data collection. The unit cell parameters and systematic absences *hkl* ($h + k = 2n + 1$) indicated three possible space groups: *C*2, *Cm*, and *C*2/*m*. A statistical analysis of intensities suggested a noncentrosymmetric space group, and the structure converged only when refined in the space group *C*2. The structure was solved by direct methods. All non-hydrogen atoms were refined anisotropically, except for the phenyl rings, which were treated as isotropic rigid groups with fixed hydrogen atoms (0.09 Å^2 fixed isotropic thermal parameters). The correct choice of enantiomer was determined in the initial stages of refinement (Mo and P anisotropic) from the value of 0.88 (near +1) for the enantiopole parameter (*η*) in the SHELXTL program package.

A red crystal of IV, shaped as an octahedron, of approximate dimensions 0.3 × 0.3 × 0.3 mm, was used for the structure determination. The unit cell parameters and systematic absences 00*l* ($l = 4n + 1, 2, 3$) and 0*k*0 ($k = 2n + 1$) indicated two possible space groups: $P4_12_12$ and $P4_32_12$. As for III, the correct enantiomorph was determined from the enantiopole parameter. The structure was solved by conventional heavy-atom methods, and successful convergence was obtained in the space group $P4_32_12$. All non-hydrogen atom thermal parameters were anisotropic except for the phenyl rings, which were treated as isotropic rigid groups. All hydrogen atoms were generated in idealized positions for the structure factor calculations but were not refined.

A green crystal of IIIa, shaped as a block, of approximate dimensions 0.2 × 0.3 × 0.4 mm, was used for the structure determination. The unit cell parameters and systematic absences *hkl* ($h + k = 2n + 1$) indicated three possible space groups: *C*2, *Cm*, and *C*2/*m*. The structure was solved by heavy-atom methods and converged well only in the space group *C*2, and it is isomorphic with III. As for III, the correct enantiomorph was determined from the enantiopole parameter. All non-hydrogen atom thermal parameters were anisotropic except for the phenyl rings, which were treated as isotropic rigid groups with fixed hydrogen atoms

(8) Chatt, J.; Leigh, G. J.; Thankarajan, N. *J. Organomet. Chem.* **1971**, *29*, 105.

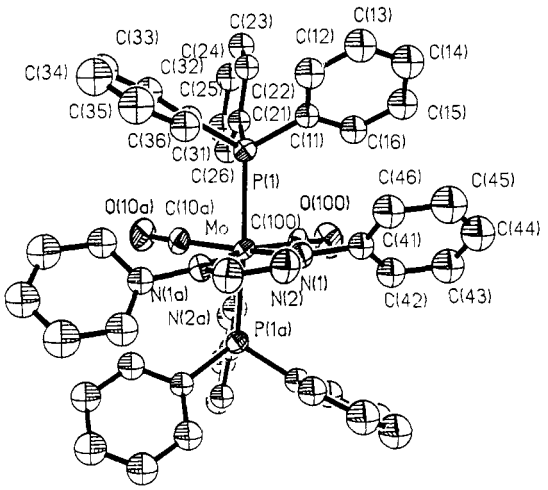

Figure 1. ORTEP plot (50% ellipsoids) and atom-labeling scheme for $Mo(1,4\text{-}Ph_2N_4)(CO)_2(PPh_3)_2$ (III). Symmetry-equivalent atoms (denoted by the letter a) are generated by the C_2 axis bisecting the metallacycle.

(0.09 Å^2 fixed isotropic thermal parameters).

A red crystal of IVa, shaped as a block, of approximate dimensions 0.2 × 0.2 × 0.4 mm, was used for the structure determination. The unit cell parameters and systematic absences $0k0$ ($k = 2n + 1$) indicated two possible space groups: $P2_1$ and $P2_1/m$. The structure was solved by the heavy-atom method and converged only in the space group $P2_1$. The structure solution posed several problems because the empirical absorption correction did not compensate well for absorption by tungsten. Overlapping enantiomeric pairs appeared in the difference Fourier map even after partial solution of the structure. This led to ambiguity in the choice of the PMe_3 ligands as cis or trans. To minimize the number of variables, only the W and P atom thermal parameters were allowed to be anisotropic and the phenyl groups were treated as rigid groups with fixed hydrogens and a common thermal parameter for each ring. The Me groups on phosphorus were also constrained to a common refined thermal parameter, since they did not refine well otherwise. The W and P atoms were refined anisotropically.

Although a cis structure solved best initially, this led to poor convergence, an unusual distorted geometry about W, and several chemically unreasonable bond distances. This suggested that the cis structure corresponded to PMe_3 ligands from opposite enantiomers. Removal of one PMe_3 ligand and a difference Fourier synthesis revealed two peaks assignable to enantiomeric phosphorus atoms. The weaker one, corresponding to a trans geometry, was selected. The resulting structure converged well (maximum shift/esd of 0.061 and mean 0.001). One large feature in the difference Fourier map, 5.3 e/Å^3, was within 1 Å of the tungsten. The data were not good enough to determine the correct enantiomer, since the enantiopole parameter was nearly zero (−0.1). We regard this as a marginal-quality structure but include it for comparison with the other complexes in the series.

Final atomic positional and isotropic thermal parameters for non-hydrogen atoms of all compounds are shown in Table II. The selected bond distances and bond angles are shown in Table III.

Results

Preparation of Mo(N(Ph)N=NNPh)(CO)$_2$(PPh$_3$)$_2$ (III). Addition of the dianionic reagent I to a benzene solution of $MoBr_2(CO)_2(PPh_3)_2$ at room temperature results in a color change from blue to red. When pentane was layered on the solution after filtration and concentration, green crystals of III formed with an equal amount of yellow crystals that proved to be *trans*-$Mo(CO)_4(PPh_3)_2$ (eq 2). The crystal structure of III (Figure 1) was de-

$$2\ trans\text{-}MoBr_2(CO)_2(PPh_3)_2 + I \rightarrow trans\text{-}Mo(CO)_4(PPh_3)_2 + III \quad (2)$$

termined through X-ray diffraction. The other product has the same melting point and ν_{CO} stretching frequencies as *trans*-$Mo(CO)_4(PPh_3)_2$, which was prepared by thermal isomerization of *cis*-$Mo(CO)_4(PPh_3)_2$.[7,8] Thus, reduction of $MoBr_2(CO)_2(PPh_3)_2$ competes with the metathetical displacement of bromide. Because we were unable to separate III from the crystal mixture, the fact[9] that trialkylphosphines have higher electron-donating power than triarylphosphines suggested to us that the reduction process might be suppressed by replacing PPh_3 with PEt_3.

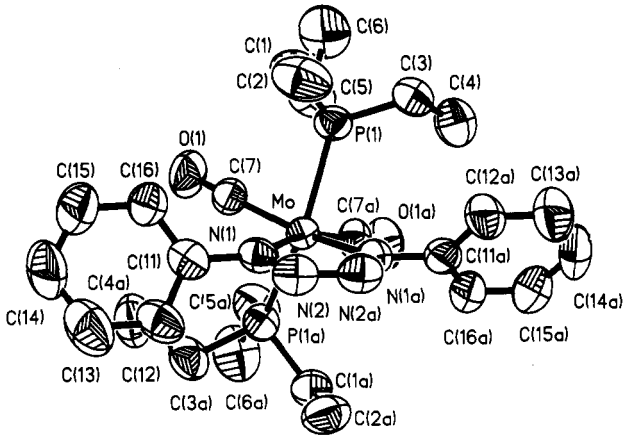

Figure 2. ORTEP plot (50% ellipsoids) and atom-labeling scheme for $Mo(1,4\text{-}Ph_2N_4)(CO)_2(PEt_3)_2$ (IV). Symmetry-equivalent atoms (denoted by the letter a) are generated by the C_2 axis bisecting the metallacycle.

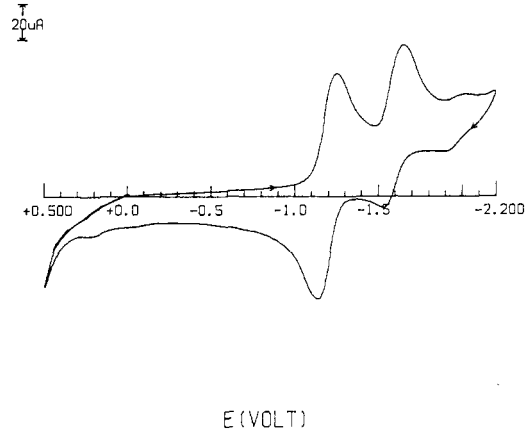

Figure 3. Cyclic voltammogram (300 mV/s scan rate) of $Mo(1,4\text{-}Ph_2N_4)(CO)_2(PEt_3)_2$ in 0.1 M $[^nBu_4N][PF_6]$–THF electrolyte solution.

Preparation and Properties of Mo(N(Ph)N=NNPh)(CO)$_2$(PEt$_3$)$_2$ (IV). Addition of I to a benzene solution of $MoBr_2(CO)_2(PEt_3)_2$ at room temperature results in a color change from blue to red. Complex IV was isolated after removal of volatiles and recrystallization from heptane (eq 3). The structure of IV was determined

$$MoBr_2(CO)_2(PEt_3)_2 + I \xrightarrow{C_6H_6} IV + 2LiBr \quad (3)$$

through X-ray diffraction (Figure 2). The electronic absorption spectrum of IV displays two energy maxima at 561 nm (ϵ = 490 M^{-1} cm^{-1}) and 461 nm (ϵ = 5800 M^{-1} cm^{-1}) (see Experimental Section).

Results of cyclic voltammetry studies on IV are shown in Figure 3. The cyclic voltammogram displays two reversible one-electron-reduction waves at −1.18 and −1.59 V vs a Ag-wire pseudo reference electrode. These results

(9) Tolman, C. A. *Chem. Rev.* **1977**, *77*, 313.

Table II. Atomic Coordinates (×10⁴) and Isotropic Temperature Factors (Å² × 10³)

	x	y	z	U(eq)[a]		x	y	z	U(eq)[a]
				$Mo(1,4\text{-}Ph_2N_4)(CO)_2(PPh_3)_2 \cdot C_6H_6$					
Mo	0	0	0	30 (1)	C(35)	−1668	−2140	1005	71 (3)
P(1)	98 (2)	548 (3)	1676 (2)	33 (2)	C(36)	−938	−1562	1288	51 (3)
C(12)	988 (3)	−1046 (7)	3714 (5)	53 (3)	C(31)	−816	−175	1442	38 (2)
C(13)	1728	−1474	4785	62 (3)	C(100)	978 (7)	1279 (11)	814 (10)	40 (7)
C(14)	2518	−985	5212	66 (3)	O(100)	1558 (5)	1983 (8)	1268 (7)	65 (6)
C(15)	2568	−67	4568	59 (2)	N(2)	420 (5)	−2934 (8)	425 (7)	49 (6)
C(16)	1828	361	3497	49 (3)	N(1)	766 (5)	−1710 (8)	744 (7)	35 (6)
C(11)	1038	−128	3070	37 (2)	C(42)	2237 (4)	−1143 (7)	1656 (5)	52 (3)
C(22)	260 (4)	2539 (6)	3087 (5)	42 (2)	C(43)	3113	−1324	2515	68 (3)
C(23)	257	3851	3406	50 (3)	C(44)	3429	−2243	3400	69 (3)
C(24)	109	4927	2710	55 (2)	C(45)	2869	−2981	3428	75 (4)
C(25)	−37	4690	1695	64 (3)	C(46)	1993	−2800	2570	60 (3)
C(26)	−34	3377	1376	46 (3)	C(41)	1677	−1881	1684	40 (3)
C(21)	114	2302	2072	36 (2)	C(1)	5000	−5648 (22)	5000	94 (6)
C(32)	−1424 (4)	635 (5)	1312 (5)	48 (3)	C(2)	5701 (11)	−6264 (19)	5942 (14)	111 (5)
C(33)	−2154	57	1029	65 (3)	C(3)	5703 (11)	−7662 (21)	5951 (15)	123 (6)
C(34)	−2276	−1330	876	75 (4)	C(4)	5000	−8379 (31)	5000	134 (9)
				$Mo(1,4\text{-}Ph_2N_4)(CO)_2(PEt_3)_2$ (IV)					
Mo	5403 (1)	5403 (1)	0	48 (1)	C(7)	5110 (4)	4332 (4)	745 (3)	68 (2)
P(1)	3875 (1)	6104 (1)	651 (1)	64 (1)	N(2)	7252 (3)	6734 (3)	240 (2)	65 (2)
C(1)	4225 (5)	6558 (6)	1590 (3)	88 (2)	N(1)	6792 (3)	5859 (3)	466 (2)	56 (1)
C(2)	5033 (5)	7337 (6)	1612 (4)	105 (3)	C(12)	8457 (3)	5114 (3)	793 (2)	81 (2)
C(3)	3217 (5)	7232 (5)	299 (3)	88 (3)	C(13)	9089	4592	1296	113 (3)
C(4)	2636 (6)	7094 (7)	−419 (4)	129 (4)	C(14)	8707	4303	1992	126 (4)
C(5)	2865 (5)	5151 (6)	819 (5)	103 (3)	C(15)	7694	4536	2186	107 (3)
C(6)	1919 (5)	5480 (8)	1233 (5)	130 (4)	C(16)	7063	5057	1683	82 (2)
O(1)	4944 (3)	3720 (3)	1201 (3)	105 (2)	C(11)	7444	5346	987	65 (2)
				$WBr_2(PMe_3)_3(CO)_2$ (IIa)					
W(1)	322 (1)	3361 (1)	3894 (1)	39 (1)	C(6)	−325 (28)	5668 (18)	3965 (8)	80 (8)
Br(1)	629 (3)	1723 (1)	4161 (1)	71 (1)	P(3)	1308 (8)	2639 (4)	3175 (2)	63 (2)
Br(2)	−2218 (3)	2741 (2)	3543 (1)	79 (1)	C(7)	3247 (35)	2445 (21)	3173 (10)	106 (10)
P(1)	2432 (7)	3436 (4)	4431 (2)	52 (2)	C(8)	503 (34)	1614 (19)	2998 (10)	95 (9)
C(1)	2110 (33)	2967 (18)	4973 (9)	85 (8)	C(9)	1074 (33)	3276 (16)	2675 (8)	80 (8)
C(2)	4150 (35)	2944 (19)	4273 (10)	96 (9)	C(10)	−567 (27)	3778 (17)	4467 (8)	68 (7)
C(3)	3038 (31)	4520 (19)	4592 (9)	97 (9)	O(10)	−1017 (23)	4044 (13)	4793 (6)	100 (6)
P(2)	−1093 (8)	4698 (4)	3709 (2)	64 (2)	C(20)	1690 (23)	4177 (13)	3662 (7)	45 (5)
C(4)	−1197 (34)	5018 (17)	3120 (9)	94 (9)	O(20)	2574 (21)	4648 (12)	3511 (5)	88 (5)
C(5)	−2995 (39)	4760 (22)	3881 (10)	115 (11)					
				$W(1,4\text{-}N_4Ph_2)(CO)_2(PPh_3)_2 \cdot C_6H_6$ (IIIa)					
W(1)	0	0	0	31 (1)	C(23)	−250	−3888	−3375	53 (4)
P(1)	−98 (2)	−576 (4)	−1665 (3)	35 (2)	C(24)	−87	−4952	−2663	58 (3)
N(2)	408 (9)	2919 (12)	406 (11)	47 (8)	C(25)	65	−4704	−1643	72 (5)
N(1)	767 (12)	1695 (16)	763 (16)	40 (10)	C(26)	55	−3392	−1336	49 (4)
C(42)	2245 (7)	1142 (11)	1662 (9)	54 (4)	C(21)	−107	−2328	−2048	37 (3)
C(43)	3122	1333	2525	65 (5)	C(32)	−1834 (6)	−381 (12)	−3495 (8)	54 (4)
C(44)	3431	2242	3414	77 (6)	C(33)	−2572	50	−4570	69 (4)
C(45)	2861	2958	3440	65 (5)	C(34)	−2513	955	−5212	69 (5)
C(46)	1983	2766	2576	55 (4)	C(35)	−1716	1430	−4781	64 (5)
C(41)	1675	1858	1687	39 (4)	C(36)	−978	999	−3706	55 (4)
C(12)	941 (6)	1519 (12)	−1292 (10)	56 (4)	C(31)	−1037	94	−3064	43 (2)
C(13)	1671	2095	−1016	75 (6)	C(10)	−980 (14)	−1280 (18)	−796 (20)	35 (11)
C(14)	2283	1286	−882	75 (6)	O(10)	−1565 (9)	−1946 (16)	−1244 (12)	68 (9)
C(15)	2165	−99	−1025	72 (4)	C(1)	5000	5332 (18)	5000	50 (5)
C(16)	1434	−675	−1301	58 (4)	C(2)	5699 (9)	6032 (18)	5947 (13)	119 (10)
C(11)	822	134	−1435	39 (2)	C(3)	5699 (11)	7430 (18)	5948 (15)	142 (13)
C(22)	−260 (6)	−2576 (9)	−3067 (7)	39 (3)	C(4)	5000	8129 (18)	5000	185 (27)
				$W(1,4\text{-}Ph_2N_4)(CO)_2(PMe_3)_2$ (IVa)					
W	1904 (1)	2500	2699 (1)	39 (1)	C(9)	−2829	5458	2401	78 (5)
P(1)	1626 (10)	3668 (9)	4660 (9)	49 (3)	C(10)	−3184	4510	3110	78 (5)
P(2)	3704 (11)	2098 (8)	1049 (8)	49 (3)	C(11)	−2329	3556	3078	78 (5)
N(1)	1064 (27)	915 (23)	2448 (23)	41 (6)	C(12)	−1119	3551	2337	78 (5)
N(2)	−319 (28)	809 (24)	2112 (25)	45 (6)	C(13)	607 (37)	2896 (34)	5841 (32)	68 (4)
N(4)	−318 (20)	2613 (39)	2247 (18)	38 (5)	C(14)	3207 (39)	4191 (36)	5530 (36)	68 (4)
N(3)	−1105 (32)	1652 (27)	2127 (28)	50 (6)	C(15)	651 (41)	4989 (37)	4599 (39)	68 (4)
C(1)	2603 (20)	−526 (17)	3388 (16)	60 (4)	C(16)	2741 (42)	1620 (36)	−338 (35)	68 (4)
C(2)	3200	−1597	3386	60 (4)	C(17)	4730 (41)	3293 (36)	480 (37)	68 (4)
C(3)	2920	−2329	2373	60 (4)	C(18)	5051 (40)	1106 (37)	1294 (38)	68 (4)
C(4)	2044	−1990	1362	60 (4)	C(19)	3544 (34)	2062 (37)	3641 (38)	81 (8)
C(5)	1447	−918	1364	60 (4)	C(20)	2372 (40)	4030 (33)	2282 (34)	55 (7)
C(6)	1727	−186	2377	60 (4)	O(1)	4443 (31)	1793 (28)	4428 (27)	80 (7)
C(7)	−764 (23)	4500 (22)	1628 (21)	78 (5)	O(2)	2662 (36)	4948 (34)	1901 (32)	98 (8)
C(8)	−1619	5453	1660	78 (5)					

[a] Equivalent isotropic U defined as one-third of the trace of the orthogonalized U_{ij} tensor.

Table III. Selected Bond Distances (Å) and Bond Angles (deg)

$Mo(1,4\text{-}Ph_2N_4)(CO)_2(PPh_3)_2$ (III)		$Mo(1,4\text{-}Ph_2N_4)(CO)_2(PEt_3)_2$ (IV)	
	Bond Distances		
Mo-P(1)	2.494 (4)	Mo-P(1)	2.478 (2)
Mo-C(100)	2.00 (1)	Mo-C(7)	1.967 (5)
C(100)-O(100)	1.15 (1)	C(7)-O(1)	1.162 (7)
Mo-N(1)	2.086 (8)	Mo-N(1)	2.076 (4)
N(1)-N(2)	1.33 (1)	N(1)-N(2)	1.348 (5)
N(2)-N(2a)	1.33 (1)	N(2)-N(2a)	1.283 (8)
N(1)-C(41)	1.46 (1)	N(1)-C(11)	1.427 (5)
	Bond Angles		
P(1)-Mo-N(1a)	154.8 (1)	P(1)-Mo-P(1a)	144.2 (1)
P(1)-Mo-C(100)	81.2 (5)	P(1)-Mo-C(7)	77.5 (2)
P(1)-Mo-N(1)	95.3 (3)	P(1)-Mo-N(1)	113.7 (1)
C(100)-Mo-C(10a)	100.9 (6)	C(7)-Mo-C(7a)	100.8 (3)
O(100)-C(100)-Mo	177.0 (9)	O(1)-C(7)-Mo	178.0 (5)
C(100)-Mo-N(1)	94.4 (4)	C(7)-Mo-N(1)	95.6 (2)
N(1)-Mo-N(1a)	70.8 (4)	N(1)-Mo-N(1a)	70.5 (2)
Mo-N(1)-N(2)	120.5 (6)	Mo-N(1)-N(2)	120.4 (3)
N(1)-N(2)-N(2a)	114.0 (4)	N(1)-N(2)-N(2a)	114.3 (2)
C(41)-N(1)-Mo	132.0 (6)	C(11)-N(1)-Mo	130.3 (3)
C(41)-N(1)-N(2)	107.2 (7)	C(11)-N(1)-N(2)	109.1 (3)
$W(1,4\text{-}Ph_2N_4)(CO)_2(PPh_3)_2$ (IIIa)		$W(1,4\text{-}Ph_2N_4)(CO)_2(PMe_3)_2$ (IVa)	
	Bond Distances		
W(1)-P(1)	2.480 (6)	W-P(1)	2.50 (1)
		W-P(2)	2.49 (1)
W(1)-C(10)	2.00 (2)	W-C(19)	1.90 (4)
		W-C(20)	1.93 (4)
C(10)-O(10)	1.14 (3)		
W(1)-N(1)	2.08 (2)	W-N(1)	2.06 (3)
		W-N(4)	2.16 (2)
N(1)-N(2)	1.35 (2)	N(1)-N(2)	1.36 (4)
N(2)-N(2a)	1.29 (3)	N(2)-N(3)	1.25 (4)
		N(3)-N(4)	1.37 (5)
N(1)-C(41)	1.45 (2)	N(1)-C(6)	1.46 (4)
		N(4)-C(12)	1.36 (5)
	Bond Angles		
P(1)-W(1)-P(1a)	153.1 (2)	P(1)-W-P(2)	139.4 (3)
N(1)-W(1)-N(1a)	71.1 (9)	N(1)-W-N(4)	70 (1)
P(1)-W(1)-C(10)	82 (1)	P(1)-W-C(19)	80 (1)
P(1)-W(1)-N(1)	107 (1)	P(1)-W-N(1)	125 (1)
C(10)-W(1)-C(10a)	101 (2)	C(19)-W-C(20)	101 (2)
O(10)-C(10)-W(1)	176 (2)	O(2)-C(20)-W	174 (3)
C(10)-W(1)-N(1)	95 (1)	C(20)-W-N(4)	97 (2)
W(1)-N(1)-N(2)	119 (2)	W-N(1)-N(2)	119 (2)
N(1)-N(2)-N(2a)	115 (1)	N(1)-N(2)-N(3)	110 (3)
C(41)-N(1)-W(1)	132 (2)	C(6)-N(1)-W	132 (2)
C(41)-N(1)-N(2)	108 (2)	C(6)-N(1)-N(2)	109 (2)
N(1)-W(1)-N(1a)	71 (1)	N(1)-W-N(4)	70 (1)
$WBr_2(CO)_2(PMe_3)_3$ (IIa)			
	Bond Distances		
W(1)-Br(1)	2.664 (3)	W(1)-Br(2)	2.679 (3)
W(1)-P(1)	2.482 (6)	W(1)-P(2)	2.482 (6)
W(1)-P(3)	2.583 (6)	W(1)-C(10)	2.00 (3)
W(1)-C(20)	1.89 (2)	C(10)-O(10)	1.13 (3)
C(20)-O(20)	1.17 (3)		
	Bond Angles		
Br(1)-W(1)-Br(2)	82.3 (1)	Br(1)-W(1)-P(1)	76.8 (1)
Br(2)-W(1)-P(1)	156.2 (2)	Br(1)-W(1)-P(2)	155.1 (2)
Br(2)-W(1)-P(2)	77.1 (2)	P(1)-W(1)-P(2)	119.6 (2)
P(1)-W(1)-P(3)	107.6 (2)	P(1)-W(1)-P(3)	110.2 (2)
Br(1)-W(1)-C(10)	95.0 (7)	Br(2)-W(1)-C(10)	96.6 (7)
P(1)-W(1)-C(10)	74.3 (7)	P(2)-W(1)-C(10)	73.9 (7)
P(3)-W(1)-C(10)	172.8 (9)	Br(1)-W(1)-C(20)	132.5 (6)
Br(2)-W(1)-C(20)	130.0 (6)	P(1)-W(1)-C(20)	73.5 (6)
P(2)-W(1)-C(20)	72.2 (6)	P(3)-W(1)-C(20)	76.0 (6)
C(10)-W(1)-C(20)	111.1 (9)	W(1)-C(10)-O(10)	177 (2)
W(1)-C(20)-O(20)	117 (2)		

indicate that complex IV can be reduced to generate stable 19-electron and 20-electron complexes. The one-electron

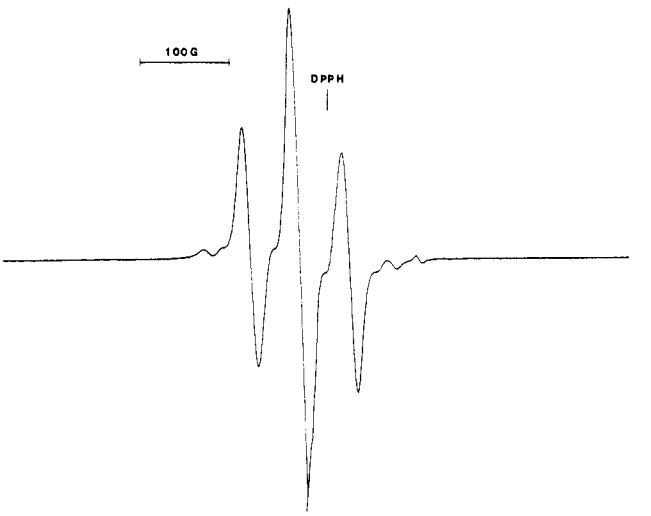

Figure 4. EPR spectrum of 10^{-3} M $[Mo(1,4\text{-}Ph_2N_4)(CO)_2(PEt_3)_2]^-$ in THF at room temperature.

character of the reduction waves was confirmed by coulometry at −1.40 V, which showed 0.72 electron per IV was transferred on reduction. The one-electron-reduced species generated in the bulk electrolysis experiment is paramagnetic. Its EPR spectrum in THF at room temperature is shown in Figure 4, which exhibits a feature at $g = 2.0215$ with hyperfine splitting assigned to $^{95,97}Mo$ and ^{31}P. The phosphorus hyperfine coupling constant ($A_P = 55.6$ G) is comparable to those found in the anionic 19-electron (diazabutadiene)molybdenum species $MoL(CO)_2(PBu_3)_2^-$ (L = $^tBuN{=}CHCH{=}N^tBu$, $A_P = 45.0$ G; L = 2,2′-bipyridyl, $A_P = 23.6$ G).[10] The reduced species is stable in THF in the absence of air, but loss of the EPR signal occurs on exposure to air. At 77 K in a THF glass the EPR spectrum does not show any additional resolved couplings. The electrochemical data prompted us to investigate the addition reaction of IV with small two-electron-donating molecules such as CO, PMe_3, and CH_3CN to see whether 20e adducts could form; however, no reaction was observed.

Preparation and Structure of $WBr_2(CO)_2(PMe_3)_3$ (IIa). Complex IIa is prepared from the reaction between $W(CO)_4Br_2$ and 3 mol of trimethylphosphine (eq 4). Moss

$$WBr_2(CO)_4 + 3PMe_3 \rightarrow IIa + 2CO \qquad (4)$$

and Shaw[6] reported the preparation of $[MX_2(CO)_2(PMe_2Ph)_3]\cdot ROH$ (M = Mo, W; X = Cl, Br; ROH = CH_3OH, C_2H_5OH) by treatment of $MX_2(CO)_4$ with 3 mol of dimethylphenylphosphine. The crystal structure of $[MoCl_2(CO)_2(PMe_2Ph)_3]\cdot CH_3OH$, shows[11] it to be mononuclear and seven-coordinate. The molecular structure with the atomic numbering scheme for IIa is shown in Figure 5. The seven-coordinate geometry can be viewed as a distorted octahedron with one additional ligand of CO (C(20)–O(20)) capping the face defined by the three PMe_3 ligands, i.e. a monocapped octahedron. Two Br atoms are located cis to each other in a distorted-octahedral unit with a Br–W–Br bond angle of 82.3 (1)°. In agreement with theoretical predictions[12] and observed patterns in seven-coordinate structures[13] the halogens lie on an uncapped

(10) tom Dieck, H.; Franz, K. D.; Hohmann, F. *Chem. Ber.* **1975**, *108*, 163.
(11) Mawby, A.; Pringle, G. E. *J. Inorg. Nucl. Chem.* **1972**, *34*, 517.
(12) Hoffmann, R.; Beier, B. F.; Muetterties, E. L.; Rossi, A. R. *Inorg. Chem.* **1977**, *16*, 511.

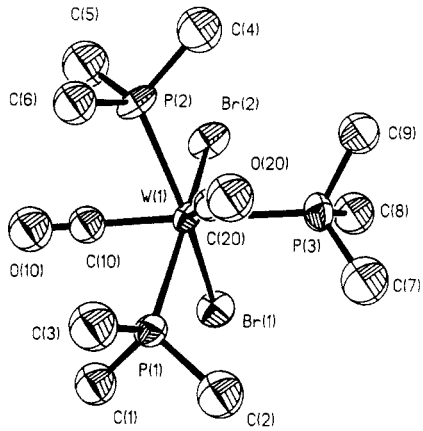

Figure 5. ORTEP plot of $WBr_2(CO)_2(PMe_3)_3$ (IIa) showing the atom-labeling scheme and 50% probability thermal ellipsoids.

face. Because of the strong trans influence of CO, the W(1)–P(3) bond distance (2.586 (6) Å) is significantly longer than those of W(1)–P(1) (2.482 (6) Å) and W(1)–P(2) (2.482 (6) Å). The bond distance of W(1)–C(10) (2.00 (3) Å) is longer than that of W(1)–C(20) (1.89 (2) Å), primarily from the trans influence of PMe_3. The Br(1), Br(2), P(1), and P(2) atoms are nearly coplanar, with the maximum displacement of an atom from the least-squares plane not exceeding 0.027 Å. The tungsten metal is located 0.336 Å from this plane. These structural data explain the ^{31}P NMR spectrum of IIa, which shows a doublet (δ −15.2, 2 P, J_{P-P} = 14.6 Hz, J_{W-P} = 155 Hz) and a triplet (δ −38.7, 1 P, J_{P-P} = 14.6 Hz, J_{W-P} = 152 Hz) with sharp satellites due to $^{183}W-^{31}P$ couplings and suggests that the seven-coordinate complex is not fluxional at room temperature. In the crystal structure of $[MoCl_2(CO)_2(PMe_2Ph)_3]$[11] there are three nonequivalent meridional PMe_2Ph ligands with P–Mo–P angles of 114.3 (4), 83.3 (4), and 156.9 (4)°, whereas complex IIa has three similar P–W–P angles of 119.6 (2), 110.2 (6), and 107.6 (2)°. The structure of IIa, however, closely resembles that of $MoBr_2(CO)_2(PMe_2Ph)_3\cdot(CH_3)_2CO$,[14] in which the three facial PMe_2Ph groups of the pseudooctahedron exhibit nearly equivalent P–Mo–P angles (107.9 (2), 111.6 (2), and 116.3 (2)°). Although the earlier workers[14] speculated that a pseudorotation in solution might interconvert the two phosphorus environments, the NMR spectral data for IIa suggest it adopts a static solution geometry.

Preparation of W(N(Ph)N=NN(Ph))(CO)$_2$(PPh$_3$)$_2$ (IIIa). Addition of the dianionic reagent I to a benzene solution of *trans*-$WBr_2(CO)_2(PPh_3)_2$ at room temperature results in a color change from blue to red. When pentane was layered on the solution after filtration and concentration, green crystals of IIIa formed with an apparently equal amount of yellow crystals of *trans*-$W(CO)_4(PPh_3)_2$ (eq 5). These results are similar to the reaction of I with

$$2\ trans\text{-}WBr_2(CO)_2(PPh_3)_2 + I \rightarrow trans\text{-}W(CO)_4(PPh_3)_2 + IIIa \quad (5)$$

the Mo analogue to produce *trans*-$Mo(CO)_4(PPh_3)_2$ and $Mo(N(Ph)N{=}NNPh)(CO)_2(PPh_3)_2$. In eq 1 *trans*-$W(CO)_4(PPh_3)_2$ is formed by reduction ($W^{2+} \rightarrow W^0$) and IIIa is formed by metathesis. Unfortunately we could only separate IIIa from the crystal mixture by hand, but X-ray diffraction proved that IIIa was indeed a tetrazene complex

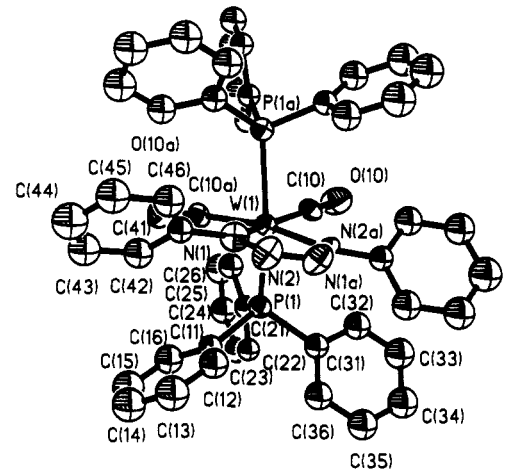

Figure 6. ORTEP plot of $W(1,4\text{-}Ph_2N_4)(CO)_2(PPh_3)_2$ (IIIa) (50% probability thermal ellipsoids). Unlabeled atoms are related to labeled atoms by the C_2 axis bisecting the metallacycle ring.

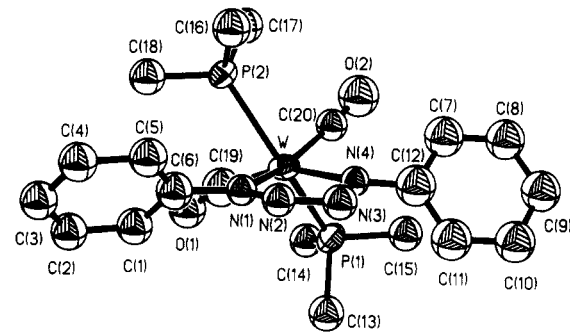

Figure 7. ORTEP plot of $W(1,4\text{-}Ph_2N_4)(CO)_2(PMe_3)_2$ (IVa) showing the atom-labeling scheme and 50% probability thermal ellipsoids.

(Figure 6). We therefore tried to employ a dihalo precursor containing trialkylphosphines to suppress the reduction process, which produced *trans*-$W(CO)_4(PPh_3)_2$ (vide infra).

Preparation and Properties of W(N(Ph)N=NNPh)(CO)$_2$(PMe$_3$)$_2$ (IVa). Addition of I to a toluene solution of IIa at room temperature results in a color change from yellow to red, and IVa was isolated after filtration and cooling to −40 °C (eq 6). The structure of

$$WBr_2(CO)_2(PMe_3)_3 + [Li(THF)_x]_2(I) \rightarrow IVa + PMe_3 + 2LiBr + x\text{THF} \quad (6)$$

IVa was determined through X-ray diffraction (Figure 7).

The cyclic voltammogram of IVa displays two chemically irreversible reductions at −1.72 and −2.16 V vs a Ag-wire pseudo reference electrode. These results contrast with those found in the reduction of $Mo(1,4\text{-}N_4Ph_2)(CO)_2(PEt_3)_2$, which show two reversible one-electron reductions at −1.18 and −1.59 V. Complex IV did not react with two-electron-donor ligands such as CO, PMe_3, and CH_3CN.

Discussion

One problem encountered in the synthesis of Mo and W tetraazabutadiene complexes by metathesis of Mo(II) and W(II) halide complexes with $Li_2N_4Ph_2$ was the competition between halide displacement and reduction of the metal center. Thus, the best results were obtained with the more electron-rich precursors $MoBr_2(CO)_2(PEt_3)_2$ and $WBr_2(CO)_2(PMe_3)_3$. The relatively low values of ν_{CO} stretching frequencies in the $M(1,4\text{-}Ph_2N_4)(CO)_2L_2$ complexes III (1826, 1925 cm^{-1}), IIIa (1817, 1918 cm^{-1}), IV (1815, 1910 cm^{-1}), and IVa (1819, 1919 cm^{-1}) suggest that

(13) Lippard, S. J. *Prog. Inorg. Chem.* **1976**, *21*, 91. Drew, M. G. B. *Prog. Inorg. Chem.* **1977**, *23*, 67. Kepert, D. L. *Prog. Inorg. Chem.* **1979**, *25*, 41.

(14) Drew, M. G. B.; Wilkins, J. D. *J. Chem. Soc., Dalton Trans.* **1977**, 557.

Table IV. Least-Squares Planes in Complexes III and IV

Least-Squares Planes

plane no.	atoms in plane	eq of plane[a] A	B	C	D	av displacement, Å
		$Mo(1,4\text{-}Ph_2N_4)(CO)_2(PPh_3)_2$ (III)				
1	MoN_4	−14.544	0	15.245	0	0.0131
2	MoP_2	16.516	0	−0.950	0	0
3	$Mo(CO)_2$	−12.231	0	15.243	0	0.0200
4	C(41)–C(46)	−9.796	6.867	11.057	−1.1099	0
5	C(41a)–C(46b)	−9.796	−6.867	11.057	1.1098	0
		$Mo(1,4\text{-}Ph_2N_4)(CO)_2(PMe_3)_2$ (IV)				
1a	MoN_4	−6.361	6.361	12.952	0	0.0113
2a	MoP_2	4.555	−4.555	15.583	0	0
3a	$Mo(CO)_2$	−8.137	8.137	8.347	0	0.0072
4a	C(11)–C(16)	3.917	11.355	6.860	9.6633	0
5a	C(11a)–C(16a)	11.355	3.916	−6.860	9.6630	0

Dihedral Angles between Planes

plane no.	plane no.	angle, deg	plane no.	plane no.	angle, deg
1	2	82.3	1a	2a	73.5
1	3	8.4	1a	3a	18.5
1	4	43.8	1a	4a	57.6
2	3	89.3	2a	3a	92.0
4	5	87.3	4a	5a	67.7

[a] The equations are of the form $Ax + By + Cz = D$.

the metal center can act as a good π donor. This may explain the high stability of these early-transition-metal tetraazabutadiene complexes. All other known transition-metal complexes containing a tetraazabutadiene ligand are found in electron-rich systems to the right of the manganese triad.

The exact electronic nature of the $M(1,4\text{-}Ph_2N_4)(CO)_2(PR_3)_2$ complexes is more problematic. Two extreme resonance descriptions of the metallacycle are shown as A and B. In A the neutral tetraazabutadiene ligand is

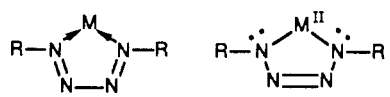

analogous to the neutral diazabutadiene ligand and III, IIIa, IV, and IVa can be regarded as 18-electron complexes. No X-ray structure of a "tetraazabutadiene" complex, including III, IIIa, IV, and IVa, has exhibited a diene structure[15] with two short and one long N–N distance, although three equivalent N–N bond lengths have been observed in III, $Ni(1,4\text{-}Ph_2N_4)(PPh_2Me)_2$,[2b] $Ni(1,4\text{-}(3,5\text{-}Me_2C_6H_3)_2N_4)_2$,[1f] and $Fe(1,4\text{-}Me_2N_4)(CO)_3$.[1g] In form B the dianionic tetrazenido ligand would result in a less satisfying 16-electron M(II) description for III–IVa, even though the X-ray structural data are more consistent with this picture. One short N–N and two long N–N distances usually have been found by X-ray diffraction studies as in IIIa, IV, IVa, $Pt(1,4\text{-}Ph_2N_4)(PEt_3)_2$,[2b] $Ir[(4\text{-}FC_6H_4)N_4(4\text{-}C_6H_4F)](CO)(PPh_3)$,[1h] $Pt(1,4\text{-}(4\text{-}NO_2C_6H_4)_2N_4)(CHC(PEt_3)H(CH_2)_2CH{=}CHCH_2CH_2)(PEt_3)$,[1i] $(HC{\equiv}C)_2(PEt_3)_2Pt[1,4\text{-}(4\text{-}NO_2C_6H_4)_2N_4]$,[1m] $(\eta^5\text{-}C_5H_5)Co(1,4\text{-}(C_6F_5)_2N_4)$,[1a] and $(\eta^5\text{-}C_5H_5)Ni(1,4\text{-}(4\text{-}MeC_6H_4)_2N_4)$.[1l]

Molecular Geometry and Bonding. The molecular structures of III, IIIa, IV, and IVa (Figures 1, 2, 6, and 7) all have a C_2 axis passing through the metal, bisecting the N(2)–N(2a) or N(2)–N(3) bonds. For III, IIIa, and IV the C_2 axis is crystallographically imposed. The coordination spheres of all complexes can be described as distorted octahedrons, with an equatorial plane formed by two carbonyl carbon atoms and two terminal nitrogen atoms. The bulkier phosphine groups occupy the less hindered axial positions. In all complexes the metallacycle ring adopts a nearly planar geometry with the maximum displacement of an atom from the least-squares planes not exceeding 0.036 Å (Tables IV and V). All phenyl rings on the metallacycles are twisted out of the plane of the metallacycle ring and are mutually perpendicular (68–87°) (Tables IV and V). The opposing cant of the phenyl rings imparts chirality to the structure and may explain the tendency (Table I) of these compounds to crystallize in acentric space groups. Given the low-lying charge-transfer transitions associated with the tetraazabutadiene metallacycle, these compounds may be candidates for nonlinear optical materials.

In Table VI are summarized metrical parameters important in characterizing metallacycle bonding. In III all three N–N distances are equivalent and the departure from a pseudooctahedral structure is small as judged by the ϕ value (MN_4–MP_2) of 82.3°. Because the MP_2 and $M(CO)_2$ planes are at nearly right angles to each other in III (89.3°), IIIa (88.9°), IV (92.0°), and IVa (91.9°), the ϕ dihedral angle between the MP_2 and metallacycle planes provides a convenient gauge of distortion. Of particular significance is the decrease of ϕ from the ideal value of 90° as the size of the phosphine ligand decreases: III, IIIa → IV → IVa. The PPh_3, PEt_3, and PMe_3 ligands have respective cone angles of 145, 132, and 118°.[9] This inverse relation between the ligand size and the structural distortion (i.e. less sterically crowded complexes show more distortion) suggests that electronic factors favor the distortion and it increases as permitted by the decreasing size of the phosphine ligands. The effect of the distortion, which removes the two carbonyl groups from coplanarity with the metallacycle, by as much as 30° in IVa, is to reduce competition between the N_4Ph_2 and two CO ligands for π-electron density on the metal. This would be consistent with the picture of

(15) For examples of expected N—N and N=N bond lengths, see: (a) *trans*-tetrazene, $H_2NN{=}NNH_2$ (N—N = 1.41 (1) Å; N=N = 1.21 (2) Å): Veith, M.; Schlemmer, G. *Z. Anorg. Allg. Chem.* **1982**, *494*, 7. (b) tetrakis(trimethylsilyl)tetrazene, $(Me_3Si)_2NN{=}NN(SiMe_3)_2$ (N—N = 1.394 (5) Å; N=N = 1.268 (7) Å): Veith, M. *Acta Crystallogr., Sect. B* **1975**, *31*, 678–684.

Table V. Least-Squares Planes for IIIa and IVa

Least-Squares Planes

plane no.	atoms in plane	eq of plane[a] A	B	C	D	av displacement, Å
		$W(1,4\text{-}Ph_2N_4)(CO)_2(PPh_3)_2$ (IIIa)				
1	WN_4	−15.074	0	15.157	0	0
2	WP_2	16.477	0	−0.970	0	0
3	$W(CO)_2$	−12.165	0	15.215	0.0000	0.012
4	C(41)–C(46)	8.681	7.271	−10.437	1.0441	0
5	C(41a)–C(46a)	−8.681	7.271	10.437	1.0441	0
		$W(1,4\text{-}Ph_2N_4)(CO)_2(PMe_3)_2$ (IVa)				
1a	WN_4	−1.928	−0.686	10.269	2.2256	0.0346
2a	WP_2	−3.320	8.939	−5.800	0.0371	0
3a	$W(CO)_2$	−4.548	3.998	8.569	2.4307	0.0528
4a	C(1)–C(6)	7.597	4.239	−5.162	0.0059	0
5a	C(7)–C(12)	4.950	4.165	8.054	2.8068	0

Dihedral Angles between Planes

plane no.	plane no.	angle, deg	plane no.	plane no.	angle, deg
1	2	79.8	1a	2a	58.7
1	3	10.9	1a	3a	29.5
1	4	47.5	1a	4a	49.3
2	3	89.4	2a	3a	91.9
4	5	86.4	4a	5a	80.2
			1a	5a	50.7

[a] The equations are of the form $Ax + By + Cz = D$.

Table VI. Bond Distances within the Metallacycle in III, IIIa, IV, and IVa and the Dihedral Distortion Angle from an Octahedral Environment

complex	M–N, Å	av N(1)–N(2) and N(3)–N(4), Å	N(2)–N(2a) or N(2)–N(3), Å	$\phi(MN_4\text{-}MP_2)$, deg
III	2.086 (8)	1.33 (1)	1.33 (1)	82.3
IIIa	2.08 (2)	1.5 (2)	1.29 (3)	79.8
IV	2.076 (4)	1.348 (5)	1.283 (8)	73.5
IVa	2.06 (3)	1.36 (4)	1.25 (4)	58.7
	2.16 (2)	1.37 (5)		

these compounds as 18-electron complexes where $d\pi \rightarrow N_4\ \pi^*$ back-bonding is extensive.

The other distortion that occurs in these systems is the OC–M–CO angle opens to ~100° in III–IVa and the P–M–P angle decreases from 180° (140–155°). Kepert[16] has examined the systematics of L–M–L bond angle changes in octahedral complexes and has shown that chelates with a normalized bite[16] less than $2^{1/2}$ lead to an opening of the in-plane trans L–M–L angle from 90° and a closing of the perpendicular L′–M–L′ angle from 180°. Since the normalized bite of the $1,4\text{-}Ph_2N_4$ ligand in III–IVa ranges from 1.15 to 1.26, the OC–M–CO and P–M–P angular distortions follow the known trend. The small N–M–N angle (70.5–73.5°) in these compounds results from the unusually small bite of the N_4Ph_2 chelate.

The EPR spectroscopic data for IV^- resemble those of the radical anion $Mo(DAB)(CO)_2(PBu_3)_2^-$, where DAB = (^{t}Bu)N=CHCH=N(^{t}Bu). The magnitude of the phosphorus hyperfine splitting in these radicals have been shown to correlate with the π-acceptor ability of the diimine ligand.[10] Since A_P for IV^- is 10 G larger than for the DAB analogue, this is consistent with an exceptional π-acceptor ability for the tetraazabutadiene ligand.

Although the electrochemical data for III–IVa show an ability to successively add two electrons at moderate potentials, the complexes do not react with two-electron-donor ligands. This suggests that reduction results in occupation of a metallacycle π orbital as observed in late-transition-metal complexes.[1e,l] Two-electron reduction can also be viewed as resulting in a transformation to the valence bond scheme B described earlier. This further underscores the flexible redox character of these complexes and the utility of both resonance forms A and B in discussing the bonding and reactivity of metal tetraazabutadiene complexes.

Acknowledgment. This work is based on research sponsored by the Air Force Office of Scientific Research, Air Force System Command, USAF, under Grant AFOSR-86-0027. We thank the DoD University Research Instrumentation Program (Grant DAAL03-87-G-0071) for funds to purchase an X-ray diffractometer.

Registry No. $[Li]_2I$, 109719-17-7; II, 25685-65-8; IIa, 126186-29-6; III, 126083-41-8; IIIa, 126109-73-7; IV, 126083-42-9; IVa, 126083-43-0; *cis*-$Mo(CO)_4(NHC_5H_{10})_2$, 65337-26-0; *cis*-$Mo(CO)_4(PEt_3)_2$, 19217-80-2; $MoBr_2(PPh_3)_2(CO)_2$, 15691-85-7; $W(CO)_6$, 14040-11-0; $WBr_2(CO)_2(PPh_3)_2$, 18973-51-8.

Supplementary Material Available: Tables of positional parameters for hydrogen atoms, thermal parameters, and bond distances and bond angles (11 pages); listings of observed and calculated structure factors (44 pages). Ordering information is given on any current masthead page.

(16) Kepert, D. L. *Prog. Inorg. Chem.* **1977**, *23*, 1. The normalized bite of a chelate is defined as the distance between donor atoms divided by the M–donor atom distance.